Eur. J. Mineral.
2019, **31**, 595–608
Published online 2 April 2019

Oyelite: new mineralogical data, crystal structure model and refined formula $Ca_5BSi_4O_{13}(OH)_3 \cdot 4H_2O$

Igor V. PEKOV[1,2,*], Natalia V. ZUBKOVA[1], Nikita V. CHUKANOV[3], Vasiliy O. YAPASKURT[1], Sergey N. BRITVIN[4], Anatoly V. KASATKIN[5] and Dmitry Y. PUSHCHAROVSKY[1]

[1]Faculty of Geology, Moscow State University, Vorobievy Gory, 119991 Moscow, Russia
*Corresponding author, e-mail: igorpekov@mail.ru
[2]Vernadsky Institute of Geochemistry and Analytical Chemistry, Russian Academy of Sciences, Kosygina Str. 19, 119991 Moscow, Russia
[3]Institute of Problems of Chemical Physics, Russian Academy of Sciences, 142432 Chernogolovka, Moscow region, Russia
[4]Department of Crystallography, St Petersburg State University, Universitetskaya Nab. 7/9, 199034 St Petersburg, Russia
[5]Fersman Mineralogical Museum of Russian Academy of Sciences, Leninsky Prospekt 18-2, 119071 Moscow, Russia

Abstract: Oyelite from the Bazhenovskoe deposit, Central Urals, Russia, and the N'Chwaning Mines, Kalahari, South Africa, was studied using electron microprobe, X-ray diffraction (XRD) and infrared spectroscopy, and published data on this mineral were revisited. The crystal structure of oyelite was determined for the first time, on sample from Bazhenovskoe (single-crystal XRD, R = 12.01%). The mineral is triclinic, P-1, a = 7.2557(5), b = 10.7390(11), c = 11.2399(8) Å, α = 89.432(7), β = 89.198(6), γ = 72.097(8)°, V = 833.30(12) Å^3 and Z = 2. Oyelite represents a unique, novel structure type. Two different kinds of tetrahedral units with different topology, both linear and running along [100], occur in the structure: (I) the borosilicate chain $[BSi_2O_7(OH)_2]^{\infty}$ consisting of Si_2O_7 disilicate groups connected *via* single $BO_2(OH)_2$ tetrahedra, and (II) the interrupted chain ("dotted line") formed by $Si_2O_6(OH)$ disilicate groups bonded to each other by very strong H-bonds. The tetrahedral units I and II are linked to (010) layers of seven-fold coordinated Ca polyhedra of three different types: $CaO_6(H_2O)$, $CaO_3(H_2O)_4$ and CaO_6OH. The crystal chemical formula of oyelite is $Ca_5[BSi_2O_7(OH)_2][Si_2O_6(OH)] \cdot 4H_2O$ and the refined idealized formula is $Ca_5BSi_4O_{13}(OH)_3 \cdot 4H_2O$. Taking into account published chemical data for samples from two Japanese localities showing that oyelite may contain sligthly more H_2O, its general simplified formula could be $Ca_5BSi_4O_{13}(OH)_3 \cdot 4–5H_2O$. The powder X-ray diffraction (PXRD) pattern of oyelite has been refined and the reflections re-indexed. Oyelite demonstrates common crystal-chemical features with vistepite in part of the tetrahedral BSiO-chain and with some Ca-rich silicates, first of all with tobermorite-supergroup members, in the structure of the layered motif built of Ca-centred polyhedra and the possible occurrence of OD phenomena.

Key-words: oyelite; hydrous calcium borosilicate; tobermorite; vistepite; single tetrahedral borosilicate chain; crystal structure; Bazhenovskoe chrysotile asbestos deposit; N'Chwaning Mines.

1. Introduction

Oyelite is a hydrous calcium borosilicate with a complicated history of identification. This mineral is not very rare; rich and spectacular oyelite specimens from South Africa are well-known and adorn many collections. However, until now the crystal structure of oyelite remained unstudied, due to the poor quality of single crystals. Moreover, the symmetry, unit-cell dimensions and crystal-chemical formula of this mineral and its relationship to other mineral species have been open to question for many years.

In 2017, we identified oyelite in specimens from the Bazhenovskoe chrysotile asbestos deposit in Central Urals, Russia, and found crystals that, although not perfect, were suitable for single-crystal X-ray diffraction (XRD) study. Samples of oyelite from the N'Chwaning Mines in Kalahari, South Africa, were studied for comparison. In this paper we present novel information on oyelite, including chemical and IR spectroscopy data and a model of the crystal structure which result in refined formula and crystallographic characteristics.

2. Background information

First data on the mineral now known as oyelite were published by Heller & Taylor (1956). It was reported from the Crestmore quarries, Crestmore, Riverside Co., California, USA, as "the 10 Å hydrate" related to tobermorite.

0935-1221/19/0031-2848 $ 6.30
https://doi.org/10.1127/ejm/2019/0031-2848

The relationship between this phase and tobermorite was considered based on semi-quantitative chemical data (both are hydrated calcium silicates, and no information on boron was reported) and some similarity of powder X-ray diffraction (PXRD) patterns, with the major difference in interplanar spacing of the strongest low-angle reflection: d = 10 Å for "10 Å hydrate" (Table 1) *vs.* 11.0–11.4 Å for "ordinary" tobermorite. The following dimensions of orthorhombic unit cell were calculated from PXRD data for "10 Å hydrate": a = 11.2, b = 7.32, c = 20.5 Å (Table 2) (Heller & Taylor, 1956). Later Murdoch (1961) mentioned that a tobermorite-like mineral from Crestmore contains several per cent of B_2O_3.

In 1980, "10 Å tobermorite" was described at the Fuka mine, Fuka, Bitchu-cho, Okayama Prefecture, Japan. Its similarity with "10 Å hydrate" from Crestmore in PXRD pattern (Table 1) was shown. However, in this hydrous calcium silicate 4.8 wt% B_2O_3 was determined (#1 in Table 3). The unit-cell dimensions calculated from PXRD data of this mineral under the assumption that it is orthorhombic were given as a = 11.25, b = 7.25, c = 20.46 Å (Table 2) (Kusachi *et al.*, 1980). The same authors (Kusachi *et al.*, 1981) described this borosilicate from Fuka (the holotype locality) and Crestmore as the new mineral oyelite, a separate species, presumably belonging to the tobermorite group. This conclusion was based on a significantly higher value of the Ca:Si ratio in comparison with tobermorite and the presence of boron (##1 and 2 in Table 3). Oyelite was approved as a valid mineral species by the IMA Commission on New Minerals and Mineral Names (IMA proposal No. 1980-103). The simplified formula was suggested as $Ca_{10}B_2Si_8O_{29}{\cdot}nH_2O$ (n = 9.5–12.5) (Kusachi *et al.*, 1981) and later modified as $1.0CaO{\cdot}0.1B_2O_3{\cdot}0.8SiO_2{\cdot}1.25H_2O$ (Kusachi *et al.*, 1984).

In 1986 oyelite was reported from another locality in Japan, namely Suisho-dani, Ise City, Mie Prefecture. For this material, quantitative chemical analysis (#3 in Table 3) and PXRD pattern (Table 1) were reported (Minakawa *et al.*, 1986). In the cited paper, the formula $Ca_{10}B_2Si_8O_{29}{\cdot}12H_2O$ was proposed, which is in use for oyelite until now.[1]

Oyelite was then reported from the Kalahari Manganese Field, South Africa, in the N'Chwaning II mine (Von Bezing *et al.*, 1991). More detailed investigation of the mineral from the N'Chwaning II mine, including XRD and Raman spectroscopy and thermal studies, in comparison with the material from Fuka, was performed by Biagioni (2011). For sample from the N'Chwaning II mine, parameters of orthorhombic or pseudo-orthorhombic sub-cell [a' = 5.578 (6), b' = 3.596(4), c' = 20.46(2) Å] were found and the simplified formula was modified as $Ca_5BSi_4O_{14}(OH){\cdot}6H_2O$ (Biagioni *et al.*, 2012).

Oyelite is a hydrothermal mineral formed in late-stage assemblages related to various geological formations. At Crestmore and Fuka, the oyelite-bearing parageneses are related to classic calcic skarns (Murdoch, 1961; Kusachi *et al.*, 1984), at Suisho-dani to rodingite embedded in serpentinite (Minakawa *et al.*, 1986) and at N'Chwaning to strata-bound manganese ores in metamorphosed volcanogenic-sedimentary rocks (Von Bezing *et al.*, 1991; Cairncross *et al.*, 1997).

The identification of oyelite from the above-mentioned four localities is confirmed by analytical data. Some other information found in literature and databases could be concerning this mineral, however, its reliability is not confirmed. For instance, 10 Å hydrous calcium silicates presumably related to tobermorite were mentioned from the Hatrurim Formation, Israel (Gross, 1977), and from Cornet Hill, Apuseni Mts., Romania (Marincea *et al.*, 2001).

The situation with the identification of oyelite is additionally complicated by the existence of "true" tobermorite 10 Å, a boron-free calcium hydrosilicate. However, this phase, synthesized in hydrothermal experiments and also known as a product of partial dehydration on heating of kenotobermorite, was never convincingly confirmed for natural samples. The works devoted to "true" tobermorite 10 Å are reviewed by Biagioni *et al.* (2012) who studied in detail the sample obtained through heating of kenotobermorite from N'Chwaning II. One of the conclusions of the cited paper states that oyelite cannot be a natural counterpart of tobermorite 10 Å because of serious differences in chemistry (including the Ca:Si ratio: in all tobermorite-group minerals, Si > Ca in atom proportions: Biagioni *et al.*, 2015), PXRD patterns and Raman spectra. In particular, it was shown that oyelite and tobermorite 10 Å, even having similar dimensions of unit cells (sub-cells), distinctly differ in their PXRD pattern (Biagioni *et al.*, 2012).

The reported assumptions on the actual structure of oyelite are scarce. Maeshima *et al.* (2003) referred to a personal communication of Taylor, who supposed that oyelite has a tobermorite-like structure with the bridging tetrahedra either missing or replaced by borate groups. On the basis of Raman spectroscopy, Biagioni *et al.* (2012) suggested that the silicate chains likely occurring in oyelite are single chains, unlike tobermorite-group members which contain double Si–O chains (ribbons). Besides, they reported the thermal behaviour of oyelite, showing a shrinking of the c parameter to 9 Å, in agreement with Kusachi *et al.* (1980) and with the behaviour of "normal" tobermorite 11 Å, *i.e.*, tobermorite *sensu stricto* according to the IMA-approved nomenclature of the tobermorite group (Biagioni *et al.*, 2015).

3. Oyelite from Bazhenovskoe and N'Chwaning: occurrence and general appearance

The Bazhenovskoe deposit situated at the eastern border of the city of Asbest in Central Urals, Russia, is one of the world-largest deposits of high-quality chrysotile asbestos and is mined by several open pits since 1889. Geologically, it is related to the Bazhenovsky gabbro-harzburgite intrusion. As a mineral locality, the Bazhenovskoe deposit is mainly known due to rodingites formed as a result of

[1] The official IMA-CNMNC List of Mineral Names. http://ima-cnmnc.nrm.se/imalist.htm.

Table 1. Powder X-ray diffraction data of oyelite.

Crestmore, USA[a]		Fuka, Japan[b]		Suisho-dani, Japan[c]		N'Chwaning II, South Africa[d]		Bazhenovskoe, Russia[d]				*hkl*
I_{obs}*	d_{obs}, Å	I_{obs}	d_{obs}, Å	I_{obs}	d_{obs}, Å	I_{obs}	d_{obs}, Å	I_{obs}	d_{obs}, Å	I_{calc}**	d_{calc}, Å***	
vs	**10**	**100**	**10.23**	**90**	**10.29**	**100**	**10.23**	**71**	**10.22**	100	10.218	010
								1	7.60	2	7.583	011
		3	5.92	4	5.92	7	5.87	8	5.87	4, 5	5.913, 5.836	101, 111
		3	5.62	4	5.63	5	5.62	6	5.62	9	5.619	002
		4	5.12	3	5.12	3	5.12	4	5.11	3	5.109	020
mw	4.92	6	4.92	20	4.92	**23**	**4.923**	**29**	**4.921**	1, 25	4.936, 4.912	012, $0\bar{1}2$
						1	4.603	1	4.614	1, 2	4.641, 4.594	$0\bar{2}1$, $\bar{1}11$
mw	3.78	10	3.784	20	3.78	17	3.779	21	3.779	1, 17	3.791, 3.769	022, $0\bar{2}2$
						1	3.526	2	3.526	2	3.524	013
		25	**3.411**	15	3.41	**20**	**3.410**	**23**	**3.409**	1, 3, 6, 11	3.439, 3.436, 3.436, 3.406	$1\bar{2}1$, $2\bar{1}1$, $\bar{1}21$, 030
mw	3.34	1	3.316			6	3.306	7	3.306	3, 2, 3	3.311, 3.309, 3.299	201, 103, 113
						1	3.221			3	3.226	$\bar{2}21$
vs	**3.05**	6	3.069	**50**	**3.06**	**29**	**3.067**	**24**	**3.067**	34	3.066	212
						36	**3.030**	**38**	**3.031**	1, 43	3.030, 3.027	023, $\bar{2}12$
s	**2.93**	**60**	**2.917**	**100**	**2.917**	**90**	**2.917**	**100**	**2.917**	21, 40, 12, 2, 27	2.926, 2.921, 2.918, 2.907, 2.905	$\bar{2}02$, $03\bar{2}$, 222, $2\bar{1}1$, $03\bar{2}$
s	**2.80**	6	2.813	**40**	**2.812**	**26**	**2.812**	**42**	**2.812**	1, 26	2.810, 2.810	$\bar{2}\bar{3}1$, 004
						1	2.711	1	2.713	1	2.713	014
						3	2.660	4	2.660	3, 1	2.661, 2.657	$1\bar{3}1$, $2\bar{1}2$
						4	2.586	5	2.587	3	2.587	$\bar{2}\bar{1}3$
w	2.53	15	2.558	20	2.558	12	2.557	15	2.558	9, 2	2.555, 2.553	040, 203
						2	2.527	3	2.528	1, 2, 1	2.530, 2.524, 2.523	223, $\bar{2}03$, $\bar{2}20$
						3	2.487	3	2.497	1, 2	2.494, 2.492	041, $\bar{2}\bar{2}3$
vw	2.44	4	2.464	3	2.463	10	2.464	16	2.464	5, 1, 6	2.468, 2.462, 2.456	024, $1\bar{3}2$, $0\bar{2}4$
vw	2.31	7	2.327	3	2.325	10	2.327	12	2.327	3, 8	2.331, 2.320	$04\bar{2}$, $04\bar{2}$
						1	2.227			1	2.230	$\bar{2}\bar{4}2$
						5	2.191	3	2.193	4, 1	2.191, 2.190	204, 143
w	2.21	2	2.167	5	2.168	5	2.167	5	2.167	1, 2, 3	2.174, 2.167, 2.161	034, $\bar{2}04$, $0\bar{3}4$
						6	2.124	5	2.125	1, 11	2.123, 2.121	$\bar{1}\bar{1}5$, $\bar{2}30$
						6	2.091	4	2.092	1, 1, 1	2.098, 2.087, 2.085	$2\bar{2}3$, $\bar{2}23$, $2\bar{3}1$
mw	2.05	13	2.046	20	2.043	19	2.047	16	2.047	1, 8, 5, 12	2.052, 2.044, 2.043, 2.037	340, 050, $\bar{2}14$, 234
						4	2.026	3	2.025	2	2.024	341
						2	2.010	1	2.012	6	2.008	$\bar{2}\bar{3}4$
						2	1.987	1	1.986	4	1.986	$2\bar{3}2$
						2	1.945	2	1.944	4	1.940	252
						1	1.926	1	1.927	2	1.924	$\bar{2}\bar{5}2$
						5	1.885	4	1.884	2, 11	1.883, 1.882	$\bar{1}\bar{3}5$, $2\bar{2}4$
		2	1.872	10	1.869	9	1.872	9	1.874	8	1.872	$\bar{2}24$
						5	1.856	5	1.858	6	1.857	244
						3	1.835	3	1.835	10	1.831	$\bar{2}\bar{4}4$
s	**1.83**	2	1.814	15	1.813	11	1.814	7	1.814	17	1.813	420
						2	1.794	2	1.793	1	1.792	$\bar{2}15$
						1	1.778			1, 2	1.782, 1.775	$\bar{2}41$, 430
						1	1.761	5	1.761	3, 1	1.762, 1.755	026, $0\bar{2}6$
w	1.72					4	1.692	3	1.693	3, 1	1.695, 1.694	$2\bar{3}4$, $3\bar{2}3$
						4	1.686	1	1.691	7	1.690	$\bar{2}34$
						9	1.675	6	1.676	7, 4	1.674, 1.670	216, 254
						5	1.655	5	1.656	1, 4	1.656, 1.655	353, $\bar{2}16$
mw	1.62					11	1.642	13	1.642	5, 2, 10	1.645, 1.638, 1.637	036, $\bar{2}06$, $0\bar{3}6$
						4	1.630	4	1.631	3, 1, 1	1.633, 1.627, 1.627	062, $0\bar{6}2$, 442
						1	1.582	1	1.581	2	1.580	450
						2	1.568	2	1.568	2	1.567	117
						1	1.556			3	1.554	$4\bar{1}2$
						2	1.534	2	1.533	1	1.531	$\bar{3}33$
						2	1.528			1, 3	1.527, 1.527	345, 452
						3	1.514	3	1.514	3, 2	1.515, 1.515	046, $4\bar{5}2$
						2	1.505			1	1.504	$4\bar{1}4$

(Continued on next page)

Table 1. (Continued)

Crestmore, USA[a]		Fuka, Japan[b]		Suisho-dani, Japan[c]		N'Chwaning II, South Africa[d]		Bazhenovskoe, Russia[d]				*hkl*
I_{obs}*	d_{obs}, Å	I_{obs}	d_{obs}, Å	I_{obs}	d_{obs}, Å	I_{obs}	d_{obs}, Å	I_{obs}	d_{obs}, Å	I_{calc}**	d_{calc}, Å***	
						1	1.489	2	1.488	2	1.487	$\bar{3}\bar{6}3$
vw	1.44					3	1.461	3	1.461	1, 3	1.460, 1.460	064, 070
						1	1.438	1	1.440	1	1.434	531
						2	1.415	2	1.414	1, 2	1.415, 1.411	462, $0\bar{7}2$
mw	1.40					6	1.407	5	1.407	1, 10	1.405, 1.405	$\bar{4}\bar{6}2$, 008
						1	1.394	1	1.394	2	1.393	018
						2	1.367	2	1.367	2, 4, 2	1.369, 1.365, 1.364	$\bar{5}01$, $2\bar{5}4$, $\bar{2}54$

[a]Heller & Taylor (1956).
[b]Kusachi *et al.* (1980, 1984).
[c]Minakawa *et al.* (1986).
[d]This study.
*Intensity of reflection: vs – very strong, s – strong, mw – medium weak, w – weak, vw – very weak.
**For the calculated pattern, only reflections with intensities ≥1 are given.
***Calculated for unit-cell parameters obtained from single-crystal data.
The strongest reflections of measured XRD patterns are marked in bold type.

Table 2. Unit-cell parameters for oyelite from different localities calculated from powder X-ray diffraction data.

Locality	Crestmore	Fuka	Suisho-dani	N'Chwaning II	Bazhenovskoe
Parameters of triclinic unit cell calculated by us from powder X-ray diffraction data using *hkl* indices corresponding to the structure model reported in this work					
a (Å)	7.37(2)	7.26(4)	7.26(4)	7.27(1)	7.26(1)
b (Å)	10.49(4)	10.83(6)	10.82(6)	10.75(2)	10.76(2)
c (Å)	11.22(5)	11.26(7)	11.25(7)	11.25(2)	11.25(2)
α (°)	88.87(8)	89.7(1)	89.7(1)	89.47(4)	89.50(3)
β (°)	88.86(9)	89.3(1)	89.5(1)	89.13(3)	89.94(4)
γ (°)	74.3(1)	70.9(2)	70.9(2)	72.08(3)	72.08(4)
V (Å^3)	835(2)	836(3)	835(3)	836(1)	836(1)
Parameters of "tobermorite-type orthorhombic unit cell" calculated from powder X-ray diffraction data, as reported in original paper					
a (Å)	11.2	11.25	11.23	–	–
b (Å)	7.32	7.25	7.24	–	–
c (Å)	20.5	20.46	20.42	–	–
V (Å^3)	1681	1669	1660	–	–
Reference	Heller & Taylor (1956)	Kusachi *et al.* (1980, 1984)	Minakawa *et al.* (1986)	This work	This work

low-grade metamorphism of gabbro dikes embedded in serpentinites. More than 110 mineral species are known in the Bazhenovskoe rodingite complex; it is a source of numerous nice, museum-quality specimens of grossular, diopside, vesuvianite and many rarer minerals including zeolites and hydrous calcium silicates. Data on geology and mineralogy of Bazhenovskoe rodingites were recently summarized by Erokhin (2017). Calcium-boron mineralization is not uncommon here and is represented by widespread datolite $CaBSiO_4(OH)$ and two endemic minerals discovered in late-stage, hydrothermal associations related to rodingites, namely kasatkinite $Ba_2Ca_8B_5Si_8O_{32}(OH)_3{\cdot}6H_2O$ (Pekov *et al.*, 2013) and tatarinovite $Ca_3Al(SO_4)[B(OH)_4](OH)_6{\cdot}12H_2O$ (Chukanov *et al.*, 2016).

Oyelite is the third calcium borosilicate found in Bazhenovskoe rodingites. It was identified by us in specimens collected by local amateur mineralogists A.B. Loskutov and E.A. Novgorodova in 2012–2013 from a rodingite body uncovered in the eastern side of the Southern open pit. Oyelite occurs in close association with tatarinovite, pectolite, xonotlite and calcite in cavities of rodingite consisting of pale pinkish-orange grossular with subordinate white to pale greyish diopside. Oyelite forms elongated lamellar crystals up to 0.3 × 4 mm, divergent and combined in fan-shaped aggregates (Fig. 1) or radial rosettes up to 8 mm in diameter and their clusters up to 7 × 12 mm. Single crystals are colourless, whereas aggregates are pearly-white in colour.

Data on geology and mineralogy of the N'Chwaning iron-manganese deposit in Kalahari, South Africa, were summarized by Cairncross *et al.* (1997). We studied oyelite samples from N'Chwaning II and N'Chwaning III mines. In the sample from N'Chwaning II, divergent clusters of long-prismatic, lath-shaped oyelite crystals up to 1 mm long

Table 3. Chemical composition of oyelite.

Constituent	1	2	3	4	5	6	7	8
wt%								
Na_2O	0.1		0.01	–	–	–	–	
CaO	41.2	43.21	41.82	42.29	42.25	41.84	41.07	42.83
SrO				–	–	1.48	0.94	
B_2O_3	4.8	3.5	4.55	5.38	5.49	5.06	5.28	5.32
Al_2O_3	0.3	0.3	0.75	–	–	–	–	
SiO_2	35.3	37.85	36.06	36.65	36.28	37.03	36.59	36.71
H_2O	16.7	13.43	16.78	15.07**	15.03**	15.13**	14.94**	15.14
Total	99.5*	99.99*	100.00*	99.39	99.05	100.54	98.82	100.00
Formula calculated on the basis of $O_{13}(OH)_3$ per formula unit								
Na	0.02		0.00	–	–	–	–	
Ca	5.01	4.94	4.99	4.96	4.97	4.89	4.86	5
Sr				–	–	0.09	0.06	
B	0.94	0.68	0.88	1.02	1.04	0.95	1.01	1
Al	0.04	0.04	0.10	–	–	–	–	
Si	4.01	4.24	4.02	4.01	3.98	4.04	4.04	4
H_2O	4.82	3.51	4.73	4	4	4	4	4
ΣT	*4.99*	*4.96*	*5.00*	*5.03*	*5.02*	*4.99*	*5.05*	*5*
Ref.	[1, 2]	[2]	[3]	This work				

*Total also includes the following constituents not involved in formula calculations (wt%): #1 – H_2O^- 0.7, CO_2 0.4; #2 – MgO 0.1, CO_2 1.6; #3 – K_2O 0.01, MgO 0.02.

**Calculated for $(OH)_3(H_2O)_4$. Minakawa *et al.* (1986) noted that the analysis #3 was recalculated after the subtraction of minor hydrogrossular admixture. Formula for #2 was calculated by us after the subtraction of calcite admixture.

Dash means content below detection limit. ΣT = Si + B + Al (sum of tetrahedrally coordinated cations in italics.

1 – Fuka mine, Okayama, Japan; 2 – Crestmore, California, USA; 3 – Suisho-dani, Mie, Japan; 4, 5 – Bazhenovskoe deposit, Urals, Russia (4 – sample studied for crystal structure); 6 – N'Chwaning II mine and 7 – N'Chwaning III mine, both Kalahari, South Africa; 8 – calculated for $Ca_5BSi_4O_{13}(OH)_3{\cdot}4H_2O$.

References: [1] – Kusachi *et al.* (1980); [2] – Kusachi *et al.* (1981); [3] – Minakawa *et al.* (1986).

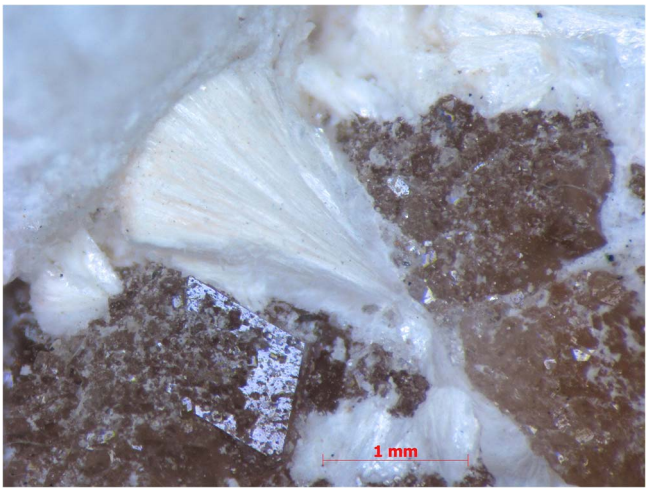

Fig. 1. Fan-shaped aggregate of oyelite with white massive tatarinovite on grossular. Bazhenovskoe deposit, Central Urals, Russia. Field of view: 4.4 mm.

(Fig. 2) occur on calcite crystal crust that covers oxide manganese ore. In the sample from N'Chwaning III oyelite forms a tight white crust up to 1 mm thick consisting of

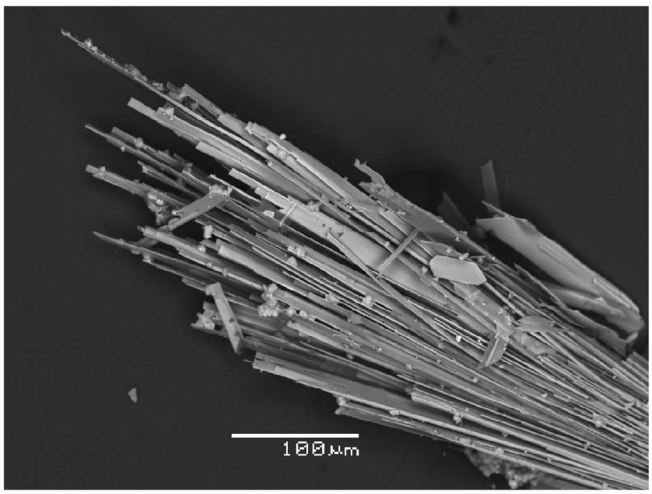

Fig. 2. Bunch of lath-shaped crystals of oyelite. N'Chwaning II mine, Kalahari, South Africa. Scanning electron microscope secondary-electron image.

radial aggregates of split acicular crystals in association with charlesite and bultfonteinite. This crust covers oxide-carbonate manganese ore mainly consisting of rhodochrosite and hausmannite.

4. Chemical composition

The chemical composition of oyelite from Bazhenovskoe deposit and N'Chwaning II and N'Chwaning III mines (##4–7 in Table 3) was studied using a Jeol JSM-6480LV scanning electron microscope equipped with an INCA-Wave 500 wavelength-dispersive spectrometer (Laboratory of Analytical Techniques of High Spatial Resolution, Dept. of Petrology, Moscow State University), with an acceleration voltage of 20 kV, a beam current of 20 nA and a beam diameter of 3 µm. The following standards were used: diopside (Ca, Si), SrF_2 (Sr) and LaB_6 (B). Contents of other elements with atomic numbers higher than oxygen are below detection limits. The absence of C- and N-bearing groups in detectable amounts is confirmed by both structure data and infrared spectrum. The H_2O content was calculated on the basis of the idealized formula $Ca_5BSi_4O_{13}(OH)_3{\cdot}4H_2O$ (#8 in Table 3) obtained from crystal-structure data (see below). The calculated H_2O content for all samples studied by us demonstrates a good agreement with the analytical totals derived from the constituents measured using the electron microprobe.

All earlier published quantitative chemical analyses of oyelite are given in Table 3 for comparison. The empirical formulae of both our and earlier studied samples were calculated on the basis of $O_{13}(OH)_3$ per formula unit (*pfu*).

Oyelite from both Japanese localities and Crestmore contains Al admixture (0.3–0.75 wt% Al_2O_3). Crestmore sample is characterized by higher Si and lower B contents. Oyelite from the N'Chwaning mines is represented by a Sr-bearing variety (0.9–1.5 wt% SrO). Samples from Fuka and Suisho-dani demonstrate some higher H_2O content compared to oyelite from other localities.

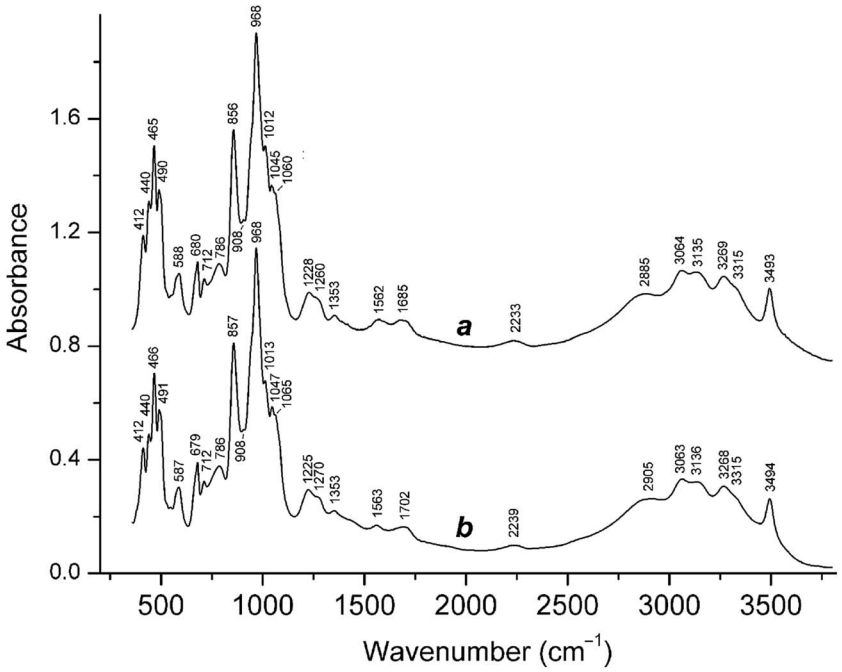

Fig. 3. Infrared absorption spectra of powdered oyelite samples from Bazhenovskoe deposit (a) and N'Chwaning II mine (b).

5. Infrared spectroscopy

In order to obtain infrared (IR) absorption spectra, powdered samples of oyelite were mixed with dried KBr, pelletized, and analyzed using an ALPHA FTIR spectrometer (Bruker Optics) with a resolution of 4 cm^{-1} and 16 scans. The IR spectrum of a pellet of pure KBr was used as a reference.

The IR absorption spectra of the oyelite samples from Bazhenovskoe deposit and N'Chwaning II mine (Fig. 3) are almost identical. Both contain bands of O–H-stretching vibrations (in the range from 2200 to 3500 cm^{-1}, including bands at 2885–2905 and 2233–2239 cm^{-1} corresponding to acid OH groups forming strong and very strong hydrogen bonds, respectively), H–O–H bending vibrations (between 1500 and 1800 cm^{-1}), B–O- and Si–O-stretching modes (in the ranges 1220–1270 and 850–1100 cm^{-1}, respectively), mixed B–O–H, Si–O–H, O–Si–O and O–B–O bending modes (bands between 500 and 800 cm^{-1}) and Si–O–Si stretching vibrations (from 400 to 500 cm^{-1}).

By analogy with the IR spectrum of the structurally related borosilicate vistepite (Chukanov, 2014), the bands at 3969–3315 and 1350 cm^{-1} are to be assigned to BO–H and SiO···H stretching vibrations, respectively.

The strongest differences between the IR spectra of the samples from Bazhenovskoe and N'Chwaning II are observed in the range from 1600 to 3000 cm^{-1}, which may be due to the shift of the dynamic equilibrium $Si–OH^{+\delta} + H_2O \leftrightarrow Si–O + H_3O^+$ or, less probably, $B–OH^{+\delta} + H_2O \leftrightarrow B–O + H_3O^+$. This phenomenon is very typical for hydrous acid salts (Chukanov & Chervonnyi, 2016).

The absence of bands corresponding to Si–O-stretching mode in the range 1100–1200 cm^{-1} indicates that Si–O–Si angles in the structure of oyelite are less than 150° (Chukanov, 2014), unlike, *e.g.*, tobermorite-type minerals showing a band in the range 1160–1200 cm^{-1} which corresponds to stretching vibrations of the linear fragment Si–O–Si connecting two neighbouring tetrahedral chains into a xonotlite-type tetrahedral Si–O ribbon.

6. X-ray crystallography and crystal-structure model

PXRD data of oyelite from Bazhenovskoe and N'Chwaning II were collected with a Rigaku R-AXIS Rapid II single-crystal diffractometer equipped with cylindrical image plate detector (radius 127.4 mm) using Debye-Scherrer geometry, Co$K\alpha$ radiation (rotating anode with VariMAX microfocus optics), 40 kV, 15 mA, and 15 min exposure. The angular resolution of the detector is 0.045 2θ (pixel size 0.1 mm). The data were integrated using the software package Osc2Tab (Britvin *et al.*, 2017). The PXRD data for both samples are given in Table 1 and compared to published data for oyelite from Crestmore, Fuka and Suisho-dani. The patterns and the unit-cell parameters derived thereof for all five samples are similar (Table 2) and undoubtedly belong to the same mineral. Intensities of reflections in PXRD diagrams of the mineral from all localities are in agreement with values calculated from the structure data obtained for the single crystal from Bazhenovskoe (Table 1).

In the frame of the "historical excursus", we also list in Table 2 dimensions of "tobermorite-type orthorhombic unit cell" reported in original papers for samples from Crestmore, Fuka and Suisho-dani.

Table 4. Crystal data, data collection information and structure refinement details for oyelite.

Formula	$Ca_5BSi_4O_{13}(OH)_3{\cdot}4H_2O$
Formula weight	654.66
Temperature (K)	293(2)
Radiation, wavelength (Å)	Mo$K\alpha$; 0.71073
Crystal system, space group, Z	Triclinic, P-1, 2
Unit-cell dimensions (Å/°)	a = 7.2557(5), α = 89.432(7) b = 10.7390(11), β = 89.198(6) c = 11.2399(8), γ = 72.097(8)
V (Å^3)	833.30(12)
Absorption coefficient (μ, mm^{-1})	2.005
F_{000}	664
Crystal size (mm)	0.07 × 0.08 × 0.12
Diffractometer	Xcalibur S CCD
θ range for data collection (°)	2.686–28.282/full sphere
Index ranges	$-9 \le h \le 9$, $-13 \le k \le 13$, $-14 \le l \le 14$
Reflections collected	11 394
Independent reflections	3914 (R_{int} = 0.2119)
Independent reflections, $I > 2\sigma(I)$	2925
Data reduction	CrysAlisPro, Agilent Technologies, v. 1.171.37.34 (Agilent Technologies, 2014)
Absorption correction	Multi-scan
Structure solution	Direct methods
Refinement method	Full-matrix least-squares on F^2
Refined parameters	246
Final R indices [$I > 2\sigma(I)$]	$R1$ = 0.1201, w$R2$ = 0.2735
R indices (all data)	$R1$ = 0.1496, w$R2$ = 0.2957
GoF	1.135
Largest diff. peak and hole (e/Å^3)	3.26 and −1.62

Table 5. Atom oordinates and equivalent displacement parameters (U_{eq}, in Å^2) for oyelite.

Site	x	y	z	U_{eq}
Ca(1)	0.5883(2)	0.58627(19)	0.87978(16)	0.0086(4)
Ca(2)	0.9219(2)	0.39635(19)	0.62176(16)	0.0092(4)
Ca(3)	0.3403(3)	0.9938(2)	0.73610(17)	0.0135(5)
Ca(4)	0.4225(3)	0.4024(2)	0.63672(16)	0.0120(4)
Ca(5)	0.9160(2)	0.41020(18)	0.13313(16)	0.0088(4)
Si(1)	0.7602(3)	0.2857(2)	0.8831(2)	0.0059(5)
Si(2)	0.1853(3)	0.2920(3)	0.8775(2)	0.0077(5)
Si(3)	0.6746(3)	0.2865(3)	0.3727(2)	0.0072(5)
Si(4)	0.2471(3)	0.3030(3)	0.3775(2)	0.0071(5)
B	0.9544(14)	0.8744(10)	0.6946(9)	0.0085(19)*
O(1)	0.1815(9)	0.3947(7)	0.2630(6)	0.0135(14)
O(2)	0.6822(9)	0.3563(7)	0.4959(6)	0.0153(14)
O(3)	0.8569(9)	0.0174(7)	0.6952(6)	0.0135(14)
O(4)	0.4860(9)	0.2252(7)	0.3733(6)	0.0108(13)
O(5)	0.1948(9)	0.3913(6)	0.4958(6)	0.0095(13)*
O(6)	0.9523(9)	0.8195(7)	0.8167(6)	0.0148(14)
O(7)	0.8448(9)	0.1469(7)	0.3479(6)	0.0138(14)
O(8)	0.6555(9)	0.3883(7)	0.2641(6)	0.0115(13)
O(9)	0.1467(9)	0.1860(7)	0.3873(6)	0.0112(13)
O(10)	0.6841(9)	0.3791(7)	−0.0045(6)	0.0120(13)
O(11)	0.6863(9)	0.3671(7)	0.7629(6)	0.0117(13)*
O(12)	0.1719(9)	0.3822(7)	0.7606(6)	0.0095(13)
O(13)	0.1805(9)	0.3815(6)	−0.0088(6)	0.0099(13)*
O(14)	0.3671(10)	0.1591(7)	0.8705(6)	0.0154(14)
O(15)	0.7036(9)	0.1494(7)	−0.1081(6)	0.0115(13)
O(16)	0.9992(9)	0.2322(7)	−0.1161(6)	0.0132(14)
O(17)	0.8430(10)	0.0337(7)	0.0905(6)	0.0164(15)*
O(18)	0.9174(9)	0.8493(7)	0.3803(6)	0.0150(14)
O(19)	0.5718(11)	0.8517(8)	−0.1293(7)	0.0237(17)
O(20)	0.4890(12)	0.8931(12)	0.3915(8)	0.043(3)

*U_{iso}.

The single-crystal XRD study of oyelite from Bazhenovskoe was carried out using an Xcalibur S diffractometer equipped with a CCD detector. A full sphere of three-dimensional data was collected. Crystal data, data collection information and structure refinement details are given in Table 4. Data reduction was performed using CrysAlisPro Version 1.171.37.34 (Agilent Technologies, 2014). The data were corrected for Lorentz and polarization effects. Empirical absorption correction using spherical harmonics, implemented in SCALE3 ABSPACK scaling algorithm, was applied. The structure was solved by direct methods and refined with the use of SHELX software package (Sheldrick, 2015) on the basis of 2925 independent reflections with $I > 2\sigma(I)$ to the final R = 0.1201. Atom coordinates and displacement parameters are presented in Table 5, selected interatomic distances in Table 6 and bond valence calculations in Table 7. Unfortunately, even the best of many tested crystals of oyelite showed low quality due to the slightly divergent character. As a result, relatively high R_{int} and final R values were obtained: 21.2% and 12.0%, respectively. Thus, we consider our results for oyelite only as a structure model. However, the reasonable values of thermal displacement parameters and interatomic distances, as well as good agreement between the measured and calculated PXRD patterns (Table 1) show that the model is correct.

The crystal structure of oyelite (Fig. 4a and b) is unique. Two different kinds of tetrahedral units, both linear and running along [100], occur in the structure (Fig. 5a). A tetrahedral unit I is the borosilicate chain $[BSi_2O_7(OH)_2]^{\infty}$ consisting of disilicate groups Si_2O_7 connected *via* single (isolated from each other) $BO_2(OH)_2$ tetrahedra. A tetrahedral unit II is the interrupted chain ("dotted line"), a motif formed by disilicate groups $[Si_2O_6(OH)]$. The general configuration of this interrupted chain is similar to that of the above-described $[BSi_2O_7(OH)_2]^{\infty}$ chain; however, B-centred tetrahedra are absent in unit II. The absence of B site leads to lowered bond-valence sum (BVS) of the O(14) site (1.31 valence units, *v.u.*, Table 7) and the presence of OH^- instead of O^{2-} in the O(15) site causes a BVS of 0.96 *v.u.* It is caused by the presence of a very strong hydrogen bond here (Fig. 5a), which is clearly confirmed by IR spectroscopic data. The distance O(14)–O(15) is 2.426(9) Å. According to Ferraris & Ivaldi (1988), this results in the increase of the BVS for O(14) up to 1.77 *v.u.* and possible H-bonding of O(14) with O(19)=H_2O. The corresponding decrease of the BVS of O(15) could be compensated by possible H-bonding with O(17)=H_2O [the O(15)–O(17) distance is 2.605(10) Å which gives a contribution of 0.28 *v.u.* to the BVS of O(15)]. As a result, the BVS for O(15)=OH is 0.78 *v.u.* Another O site with

Table 6. Selected interatomic distances (Å) in the structure model of oyelite.

Ca(1)	–O(13)	2.339(7)	Ca(5)	–O(1)	2.397(7)
	–O(10)	2.343(7)		–O(10)	2.400(7)
	–O(1)	2.353(7)		–O(6)	2.420(7)
	–O(8)	2.365(6)		–O(13)	2.425(6)
	–O(10)	2.478(7)		–O(12)	2.441(7)
	–O(11)	2.603(7)		–O(8)	2.446(7)
	–O(19)	2.817(9)		–O(13)	2.540(7)
<Ca(1)	–O>	2.471	<Ca(5)	–O>	2.438
Ca(2)	–O(12)	2.378(6)	Si(1)	–O(10)	1.604(7)
	–O(2)	2.398(7)		–O(11)	1.608(7)
	–O(11)	2.404(7)		–O(15)	1.639(7)
	–O(5)	2.405(6)		–O(16)	1.651(7)
	–O(1)	2.504(8)	<Si(1)	–O>	1.626
	–O(18)	2.535(7)	Si(2)	–O(13)	1.600(7)
	–O(5)	2.539(7)		–O(12)	1.611(7)
<Ca(2)	–O>	2.452		–O(14)	1.621(7)
Ca(3)	–O(14)	2.397(7)		–O(16)	1.664(7)
	–O(17)	2.410(7)	<Si(2)	–O>	1.624
	–O(19)	2.426(8)	Si(3)	–O(2)	1.590(7)
	–O(20)	2.431(9)		–O(8)	1.610(7)
	–O(18)	2.477(7)		–O(7)	1.646(7)
	–O(7)	2.507(7)		–O(4)	1.691(7)
	–O(4)	2.612(7)	<Si(3)	–O>	1.634
<Ca(3)	–O>	2.466	Si(4)	–O(1)	1.599(7)
Ca(4)	–O(11)	2.332(7)		–O(5)	1.613(7)
	–O(5)	2.335(7)		–O(9)	1.637(7)
	–O(12)	2.336(6)		–O(4)	1.677(7)
	–O(2)	2.379(7)	<Si(4)	–O>	1.632
	–O(8)	2.421(7)	B	–O(9)	1.459(12)
	–O(2)	2.874(8)		–O(7)	1.477(11)
	–O(20)	3.057(12)		–O(3)	1.480(12)
<Ca(4)	–O>	2.533		–O(6)	1.489(12)
			<B	–O>	1.476

relatively low BVS of 1.75 *v.u.* is O(9) and its BVS could be increased due to the H-bonding with O(18)=H_2O: the O(9)–O(18) distance is 2.691(10) Å and this results in the increase of BVS of O(9) up to 1.98 *v.u.* (Ferraris & Ivaldi, 1988).

Calcium cations occupy five crystallographically independent sites and centre seven-fold coordination polyhedra of three different types: $CaO_6(H_2O)$ for Ca(1, 2, 4), Ca(3) $O_3(H_2O)_4$ and Ca(5)O_6OH. Ca(1, 2, 4, 5)-centred polyhedra share edges to form (010) layers while isolated Ca(3)-centred polyhedra occupy the interlayer space and link adjacent layers, connecting with the polyhedra of the layers *via* common vertices (Fig. 6a). The tetrahedral units I and II are linked to the layers of Ca-centred polyhedra from both sides (Fig. 7a and b). The Ca(3)-centred polyhedra share O–O edges with the Si-centred tetrahedra of unit I and common O vertices with the Si-centred tetrahedra of unit II and each $BO_2(OH)_2$ tetrahedron shares OH-vertex [O(6)] with the Ca (5)-centred polyhedron. The H_2O groups [O(17)–O(20)] participate only in coordination of Ca cations and in the formation of H-bonds.

Thus, the structural formula of oyelite is $Ca_5[BSi_2O_7(OH)_2][Si_2O_6(OH)]\cdot 4H_2O$ and the idealized formula is $Ca_5BSi_4O_{13}(OH)_3\cdot 4H_2O$.

7. Discussion

All known natural and synthetic borosilicates with large (alkali and alkaline-earth) cations (Krzhizhanovskaya *et al.*, 2019) differ from oyelite in the topology of B–Si–O structural motifs. However, oyelite is not the first borosilicate containing infinite *dreier* single chains, with two Si-centred tetrahedra and one B-centred tetrahedron in the repeat unit (they could be also presented as formed by double tetrahedral groups Si_2O_7 and single B-centred tetrahedra): a similar tetrahedral chain was reported for vistepite. This mineral was originally described as a monoclinic borosilicate with the simplified formula $Mn_5SnB_2Si_5O_{20}$ (Pautov *et al.*, 1992) and later redefined, in accordance with crystal-structure data, as triclinic (*P*-1) $SnMn_4B_2Si_4O_{16}(OH)_2$ (Hybler *et al.*, 1997). In vistepite one vertex of the B-centred tetrahedron is protonated: $BO_3(OH)$, unlike oyelite containing the $BO_2(OH)_2$ tetrahedron. The formula of the tetrahedral chain in vistepite is, thus, $[BSi_2O_8(OH)]^{\infty}$ (Fig. 5b) *vs.* $[BSi_2O_7(OH)_2]^{\infty}$ in oyelite (Fig. 5a).

Topologically the same chains with all tetrahedra centred by Si atoms, $[Si_3O_9]^{\infty}$ are well-known in wollastonite-like pyroxenoids (Ohashi & Finger, 1978). Some minerals with wollastonite-type tetrahedral chains contain protonated O atoms (Fig. 5c), *e.g.*, members of the series pectolite $NaCa_2Si_3O_8(OH)$ – schizolite (formerly marshallsussmanite) $NaCaMnSi_3O_8(OH)$ – serandite $NaMn_2Si_3O_8(OH)$. The careful inspection of H-bonds in silicate pyroxenoid-like structures allowed to localize the OH groups in the non-bridging vertices of double tetrahedral units Si_2O_7 within the chains. The short distances (2.44–2.49 Å) between them facilitate the formation of H-bonds (Nagashima *et al.*, 2018a).

It is also worth mentioning steedeite $NaMn_2[BSi_3O_9(OH)_2]$ (Haring & McDonald, 2014) and nolzeite $NaMn_2[BSi_3O_9(OH)_2]\cdot 2H_2O$ (Haring & McDonald, 2017), two minerals structurally related to pyroxenoids. The *dreier* silicate chains in the structures of steedeite and nolzeite are decorated by branches represented by $BO_2(OH)_2$ tetrahedra. As a result, single loop-branched *dreier* borosilicate chains $[BSi_3O_9(OH)_2]^{\infty}$ are formed (Fig. 5d). Topologically similar silicate loop-branched *dreier* chains were reported in synthetic $Li_2Mg_2[Si_4O_{11}]$ (Czank & Bissert, 1993).

The motif formed by Ca-centred polyhedra in oyelite is similar to the motifs known in some other calcium-rich silicates. The layers formed by Ca(1, 2, 4, 5)-centred seven-fold polyhedra in oyelite are topologically close to those found in the structures of tobermorite-supergroup members (Biagioni *et al.*, 2015) in which the common "complex module" consisting of such layers decorated from both sides by wollastonite-like chains was distinguished (Bonaccorsi & Merlino, 2005). In oyelite, the layers are also decorated in the same way by tetrahedral units of two types (Fig. 7a and b) which could be generally considered as wollastonite-like single chains in topology: there are borosilicate chains $[BSi_2O_7(OH)_2]^{\infty}$ (unit I) alternating with interrupted chains consisting of disilicate groups $[Si_2O_6(OH)]$ (unit II) – see above. According to Merlino *et al.* (1999, 2000, 2001), the "complex module" in tobermorite-supergroup members

Table 7. Bond valence calculations for oyelite.

	Ca(1)	Ca(2)	Ca(3)	Ca(4)	Ca(5)	Si(1)	Si(2)	Si(3)	Si(4)	B	Σ
O(1)	0.34	0.23			0.30				1.07		1.94
O(2)		0.30		0.32 0.09				1.09			1.80
O(3)=OH										0.74	0.74
O(4)			0.18					0.84	0.87		1.89
O(5)		0.30 0.21		0.35					1.03		1.89
O(6)=OH					0.29					0.72	1.01
O(7)			0.23					0.95		0.75	1.93
O(8)	0.33			0.28	0.27			1.04			1.92
O(9)									0.97	0.78	1.75
O(10)	0.34 0.25				0.30	1.05					1.94
O(11)	0.18	0.30		0.35		1.04					1.87
O(12)		0.32		0.35	0.27		1.03				1.97
O(13)	0.35				0.28 0.21		1.06				1.90
O(14)			0.30				1.01				1.31*
O(15)=OH						0.96					0.96
O(16)						0.93	0.90				1.83
O(17)=H_2O			0.29								0.29
O(18)=H_2O		0.22	0.25								0.47
O(19)=H_2O	0.11		0.28								0.39
O(20)=H_2O			0.28	0.06							0.34
Σ	1.90	1.88	1.81	1.80	1.92	3.98	4.00	3.92	3.94	2.99	

*The sum for O(14) should be significantly increased due to very strong H-bond with O(15)=OH: the distance O(14)–O(15) is 2.426(9) Å. According to Ferraris & Ivaldi (1988), this results in a BVS increase for O(14) up to 1.77; the BVS for O(15) will be increased in turn due to the H-bond with O(17)=H_2O.
Bond-valence parameters are taken from Gagné & Hawthorne (2015).

has the periodicities a ~ 11.2 and b ~ 7.3 Å; in oyelite the periodicities of the (010) layer formed by Ca-centred seven-fold polyhedra decorated by tetrahedral units are very close to these values: a = 7.26 and c = 11.24 Å (Figs. 4 and 7). This apparently determines both the a and c parameters of the oyelite unit cell and demonstrates the relationship of this borosilicate with tobermorites. This common feature definitely causes, despite the quite different character of tetrahedral units (Fig. 5a–e), the similarity of PXRD patterns of oyelite and tobermorites, which is why the former was reported as a tobermorite-like mineral in early works (Heller & Taylor, 1956; Kusachi *et al.*, 1980). So-called "tobermorite 9 Å phase", $Ca_5Si_6O_{16}(OH)_2$, obtained as a product of heating and partial dehydration of clinotobermorite or tobermorite 11 Å (Merlino *et al.*, 1999, 2000), demonstrates closer structural similarity with oyelite. In "tobermorite 9 Å phase", the layers of Ca-centred polyhedra are contiguous and connected to each other through wollastonite-type single chains derived from decondensation (as a result of heating) of the typical tobermorite-like double chains (Fig. 4e and f).

Topologically similar layers of seven-fold coordinated Ca polyhedra were also reported in the structures of some other Ca-rich silicates. In fukalite $Ca_4Si_2O_6(OH)_2(CO_3)$ the calcium polyhedral framework is formed by tobermorite-type layers alternating with tilleyite-type zigzag Ca-polyhedral layers (Merlino *et al.*, 2009). Tobermorite-like layers of Ca-centred polyhedra are decorated on both sides by isolated disilicate groups $[Si_2O_7]$ in dovyrenite $Ca_6Zr[Si_2O_7]_2(OH)_4$ (Kadiyski *et al.*, 2008). In dovyrenite and structurally related disilicates (see below), $[Si_2O_7]$ groups are not connected to each other and form an interrupted chain somewhat similar to the tetrahedral unit II in oyelite (Fig. 5a). Roumaite $(Ca,Na,\square)_3(Ca,REE,Na)_4(Nb,Ti)[Si_2O_7]_2(OH)F_3$, a mineral related to dovyrenite, shows a similar motif formed by seven-fold polyhedra occupied by Ca, Na and REE, which is decorated by $[Si_2O_7]$ groups (Biagioni *et al.*, 2010), as well as other rinkite-like disilicates (*e.g.*, Pautov *et al.*, 2019).

A unique and most interesting feature of oyelite structure is the presence of two different types of tetrahedral units, both linear and elongated in the same direction. They are the "regular" borosilicate chain $[BSi_2O_7(OH)_2]^{\infty}$ (unit I) and the uncommon "dotted line" consisting of insular disilicate groups $[Si_2O_6(OH)]$, which can be considered as an interrupted chain (unit II) due to the presence of strong H-bonds [O(15)H···O(14)] linking adjacent tetrahedral islands. In the topological aspect, unit II can be presented as a derivative of unit I from which B-centred tetrahedra were "removed" (Fig. 5a). With respect to topology of the tetrahedral motif, oyelite, a mineral containing both wollastonite-like single chains and disilicate groups, could be considered as "the intermediate link" between inosilicates with wollastonite-type chains and sorosilicates with isolated disilicate groups.

The discovery of such unusual tetrahedral motif in oyelite came as a surprise and we carefully checked the correctness of the structure model – which is confirmed by two independently established facts: (1) in oyelite the atomic ratio Si:B determined by wet-chemical (literature data) and electron-microprobe (our data) methods is close to 4:1 (Table 3) whereas in vistepite, a mineral with only $[BSi_2O_8(OH)]^{\infty}$ tetrahedral chains, the atomic ratio Si:B is close to 2:1; (2) the IR spectrum confirms the presence of the strongly acidic HSi_2O_7 group forming strong hydrogen bonds (the band at

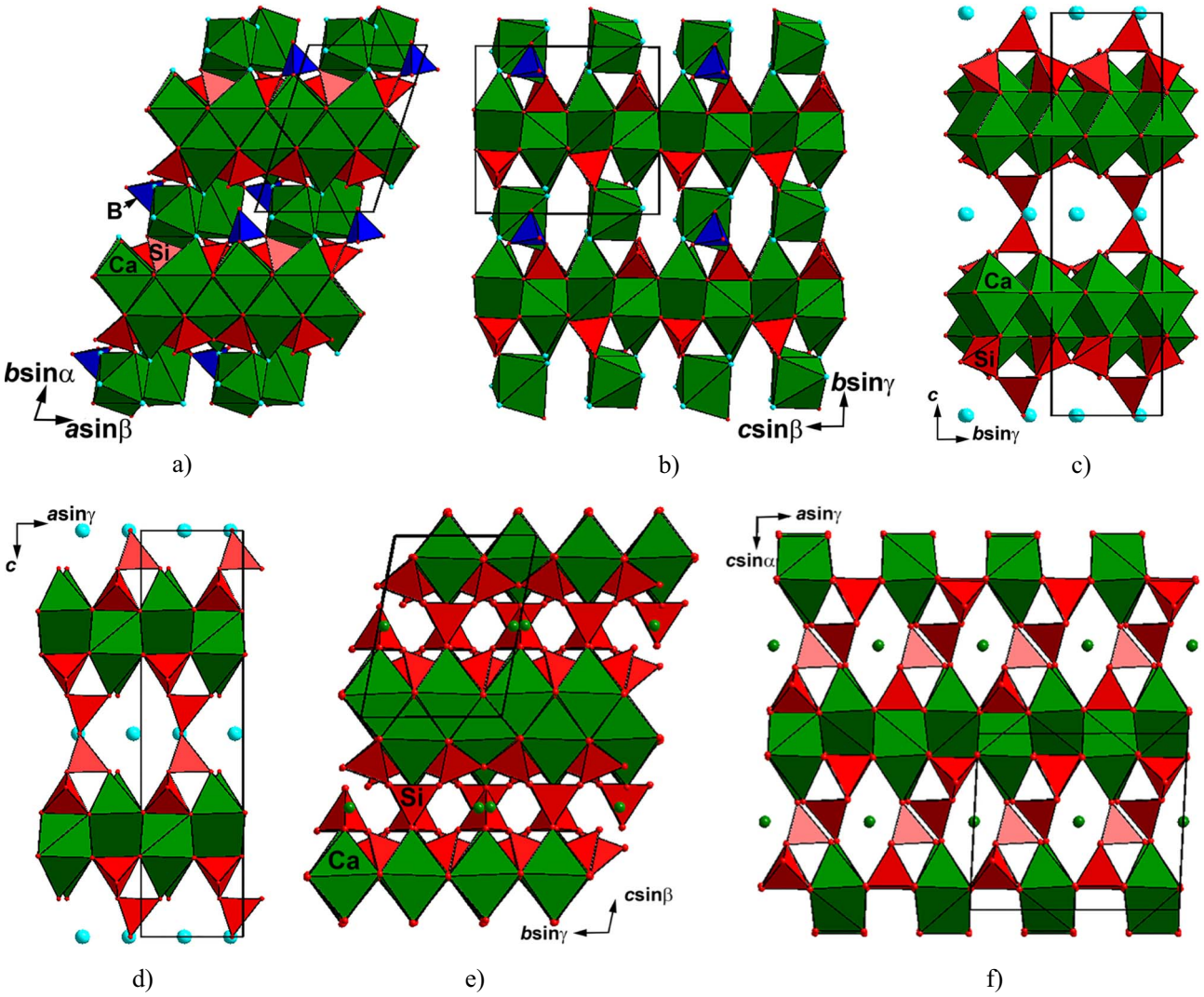

Fig. 4. The crystal structure of oyelite projected along the *c* (a) and the *a* (b) axes, the crystal structure of tobermorite 11 Å (after Merlino *et al*., 1999) projected along the *a* (c) and the *b* (d) axes, and the crystal structure of "tobermorite 9 Å phase", a product of heating of clinotobermorite or tobermorite 11 Å (with interlayer Ca cations shown as green circles; drawn after Merlino *et al*., 2000) projected along the *a* (e) and the *b* (f) axes. Positions of O atoms of H_2O groups are shown as blue circles and positions of O atoms of OH groups and O^{2-} sites as red circles. The unit cells are outlined.

2233–2239 cm^{-1}; protonated silicate or borosilicate tetrahedral chains do not show distinct bands in this region: Chukanov, 2014; Chukanov & Chervonnyi, 2016).

We have also checked the assumption that the unit cell of oyelite could be orthorhombic or pseudo-orthorhombic, with α, β and γ angles close to 90° and doubled *b* parameter, as was supposed in previous works based on PXRD data. Indeed, the unit cell of this type can be derived from the cell obtained from single-crystal data (Table 4) using the transition matrix [1 0 0/0 0 −1/−1 2 0]. Parameters of this triclinic unit cell calculated and refined for the sample from Bazhenovskoe using the same set of single-crystal data are: a = 7.2530(4), b = 11.2342(6), c = 20.4343(17) Å, α = 90.303(6), β = 91.884(6), γ = 90.815(5)° and V = 1663.93(19) $Å^3$. The structure model of oyelite obtained based on this unit cell (space group *P*-1, Z = 4) is approximately the same as the one described above. Some insignificant differences were revealed in the arrangement of water molecules involved in Ca cations coordination (however, we cannot exclude that the difference is caused by the moderate quality of the experimental data). This model is characterized by significantly higher R [0.228 for 6293 unique reflections with $I > 2\sigma(I)$], poor values of displacement parameters of almost all atoms, including negative ones for several Ca and all Si atoms. All these facts legitimate our choice of the crystal-structure model described in the present paper. Data on the structure model with the pseudoorthorhombic cell are given as Supplementary Material (Tables S1 and S2; Fig. S1) linked to this article and freely available at https://pubs.geoscienceworld.org/eurjmin/. The similarity between tobermorite-supergroup minerals and oyelite and the layered character of the structure of the latter allow one to assume the occurrence of OD phenomena, as indicated by the presence of family

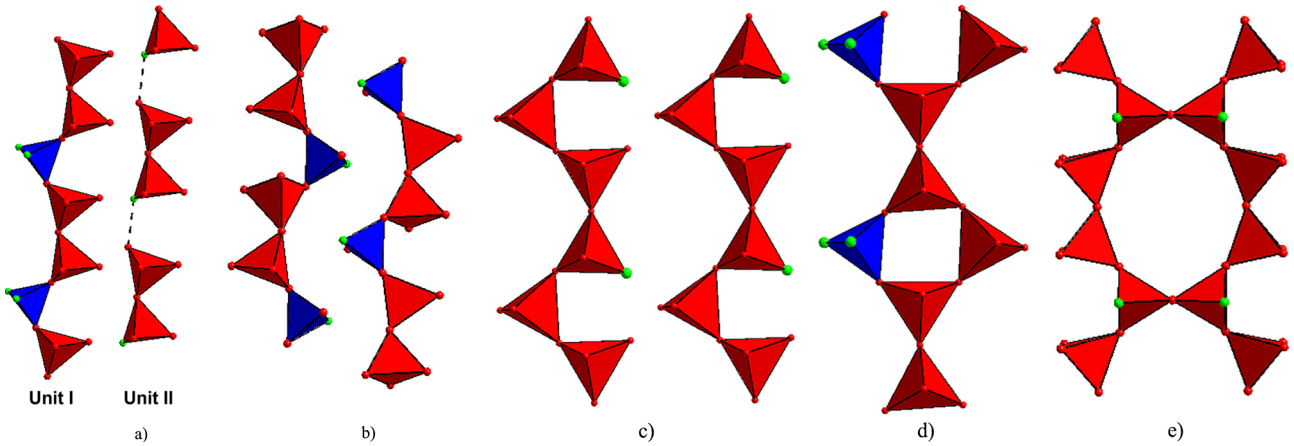

Fig. 5. Tetrahedral motifs in oyelite (a), vistepite (b, after Hybler *et al*., 1997), pectolite (c, after Arakcheeva *et al*., 2007), steedeite (d, after Haring & McDonald, 2014) and tobermorite 11Å (e, after Merlino *et al*., 1999). Si-centred tetrahedra are red and B-centred tetrahedra are blue. Positions of O atoms of OH groups are shown as small green circles. Strong H-bond between O(15)=OH and O(14) in oyelite is shown as dotted line.

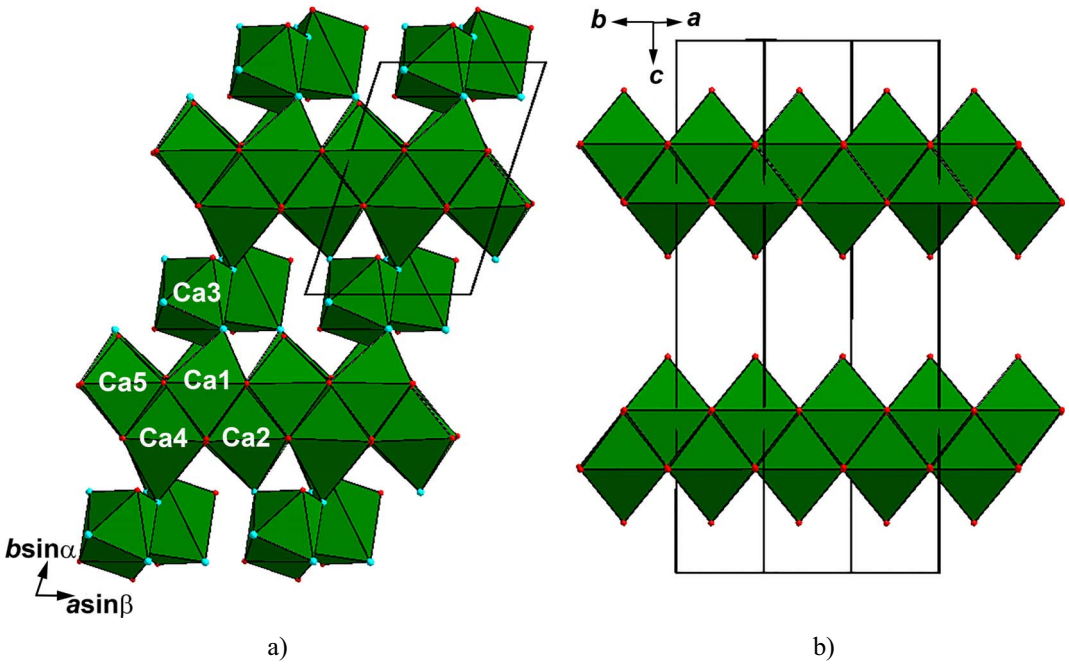

Fig. 6. Motif of Ca-centred polyhedra in oyelite (a) and tobermorite 11Å (b, after Merlino *et al*., 1999). The unit cells are outlined. Legend as in Fig. 4.

reflections reported by previous authors for oyelite (*e.g*., Biagioni *et al*., 2012). We do not observe clear signs of this for the studied sample from the Bazhenovskoe deposit; however, it seems probable that the mineral from other localities can contain two MDO (maximum degree of order) polytypes, as known for tobermorites (Merlino *et al*., 1999, 2000, 2001). Besides, it cannot be excluded that the high value of R_{int} = 21.2% for the single crystal of oyelite studied here (Table 4) can be caused, in addition to poor crystal quality, by the presence of another polytype of the mineral.

The atomic ratio Ca:Σ*T* ≈ 5:5 = 1.00 (Σ*T* = Si + B + Al, sum of tetrahedrally coordinated constituents) for all analyzed samples of oyelite well corresponds to the idealized formula $Ca_5BSi_4O_{13}(OH)_3{\cdot}4H_2O$. Noteworthy is the distinct negative correlation between B and (Si + Al) contents in Al-bearing samples from Fuka, Suisho-dani and Crestmore (Table 3). This could indicate partial substitution of B for Si with admixed Al. The substitution schemes involving silicon for compensation of boron deficiency can be assumed as follows: $Si^{4+} + OH^- \rightarrow B^{3+} + H_2O^0$ and/or $Si^{4+} + O^{2-} \rightarrow B^{3+} + OH^-$ in which the substitution OH^- for H_2O^0 could occur in the Ca(5)O_6OH polyhedron and O^{2-} for OH^- in the Ca(1, 2, 3, 4)-centred polyhedra. The scheme $Si^{4+} + O^{2-} \rightarrow B^{3+} + OH^-$ seems more probable for the sample

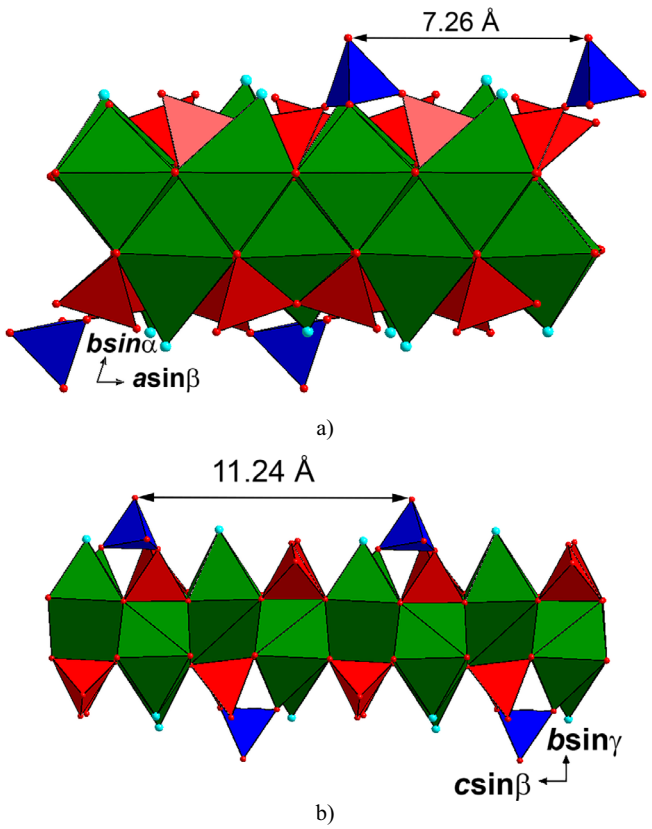

Fig. 7. The layer of Ca-centred polyhedra decorated by Si- and B-centred tetrahedra in the structure of oyelite. Legend as in Fig. 4.

from Crestmore reported by Kusachi *et al.* (1981, 1984): it contains the lowest amounts of both B and H_2O among all studied samples of oyelite (#2 in Table 3).

The phenomenon of protonation of O vertices in insular Si_2O_7 groups is rare in minerals. Earlier $[Si_2O_6(OH)]$ groups were found in davreuxite $MnAl_6Si_4O_{17}(OH)_2$ (Sahl *et al.*, 1984) and pumpellyite-type minerals (Artioli *et al.*, 2003; Lykova *et al.*, 2018; Nagashima *et al.*, 2018b). Double-protonated tetrahedral groups $[Si_2O_5(OH)_2]$ were reported for suolunite $Ca_2[Si_2O_5(OH)_2]\cdot H_2O$ (Ma *et al.*, 1999) and aklimaite $Ca_4[Si_2O_5(OH)_2](OH)_4\cdot 5H_2O$ (Zubkova *et al.*, 2012).

The Si(1)–O(16)–Si(2) angle in the disilicate group of tetrahedral unit II is 139.0(5)°, in good accordance with values commonly observed for silicates, in which frequency distributions of angles at the bridging O atoms have three maxima at 139, 157 and 180° (Baur, 1980). Comparing *T*–O–*T* angles (*T*=Si or B) in the chains of unit I in oyelite with those in vistepite reveals some obvious differences: in oyelite, the Si(4)–O(4)–Si(3) angle is 129.9° and in vistepite it is 148.5°, while Si–O–B angles in both minerals are much closer: in oyelite they are 128.4 and 135.2° and in vistepite 129.7 and 133.5° (Hybler *et al.*, 1997). A larger Si–O–Si angle in vistepite corresponds to higher frequencies of stretching vibrations of Si–O–Si groups (1112–1145 cm^{-1} *vs.* 1045–1065 cm^{-1} for oyelite).

The crystal-structure data show the presence of four H_2O molecules *pfu* in oyelite. However, the chemical analyses of samples from Fuka and Suisho-dani show higher water content, 4.83 and 4.75 H_2O *pfu*, respectively (##1 and 3 in Table 3). Thus, it is not excluded that the mineral could contain variable H_2O amounts, so its general simplified formula may be $Ca_5BSi_4O_{13}(OH)_3\cdot 4–5H_2O$. The surplus H_2O molecules could be located in the channels of the pseudo-framework built by Ca-centred polyhedra and tetrahedral chains (Fig. 4b) with possible coordinates (*x*, 0, 0) and (*x*, 0, 0.5).

8. Conclusion

The new data permit to redefine oyelite in revising its basic characteristics, namely the chemical formula, crystal system and unit-cell parameters, on the basis of the first crystal-structure model obtained. The PXRD pattern of oyelite has also been refined and the reflections re-indexed. The results obtained by us using different, independent methods (structure model based on single-crystal XRD studies and chemical, PXRD and IR spectroscopy data) are in good agreement with each other and with published data for this mineral (Kusachi *et al.*, 1980, 1981, 1984; Minakawa *et al.*, 1986; Biagioni *et al.*, 2012).

Thus, oyelite is a triclinic (space group *P*-1, $a = 7.26–7.27$, $b = 10.7–10.8$, $c = 11.2–11.3$ Å, $\alpha = 89.5–89.7$, $\beta = 89.1–89.9$, $\gamma = 70.9–72.1°$, $V = 833–836$ $Å^3$ and $Z = 2$) hydrous calcium borosilicate of a unique, novel structure type. Its crystal structure was solved on a sample from the Bazhenovskoe deposit, Central Urals, Russia. Two different kinds of tetrahedral units with different topology, both linear and running along [100], occur in the structure: (I) the borosilicate chain $[BSi_2O_7(OH)_2]^{\infty}$ consisting of Si_2O_7 disilicate groups connected *via* single $BO_2(OH)_2$ tetrahedra and (II) the interrupted chain ("dotted line") formed by $[Si_2O_6(OH)]$ disilicate groups bonded to each other by very strong H-bonds. The tetrahedral units I and II are linked to the (010) layers of seven-fold coordinated Ca polyhedra of three different types: $CaO_6(H_2O)$, $CaO_3(H_2O)_4$ and CaO_6OH. The crystal-chemical formula of oyelite is $Ca_5[BSi_2O_7(OH)_2][Si_2O_6(OH)]\cdot 4H_2O$ and the idealized formula is, thus, $Ca_5BSi_4O_{13}(OH)_3\cdot 4H_2O$. We assume that the general simplified formula of oyelite, taking into account previous chemical data showing that the mineral may contain sligthly much water, could be $Ca_5BSi_4O_{13}(OH)_3\cdot 4–5H_2O$. Oyelite demonstrates common crystal-chemical features with vistepite, $SnMn_4B_2Si_4O_{16}(OH)_2$, in part of the tetrahedral BSiO-chain and with some Ca-rich silicates, first of all with tobermorite-supergroup members, in the structure of the layered motif built of Ca-centred polyhedra.

Acknowledgements: We thank Maria G. Krzhizhanovskaya for helpful discussion and two anonymous referees for valuable comments. This study was supported by the Russian Foundation for Basic Research, grant 18-29-12007-mk. The technical support by the SPbSU X-Ray Diffraction Resource Center in the PXRD study is acknowledged.

References

Agilent Technologies (2014): CrysAlisPro Software system, version 1.171.37.34. Agilent Technologies UK Ltd, Oxford, UK.

Arakcheeva, A., Pattison, P., Meisser, N., Chapuis, G., Pekov, I., Thelin, P. (2007): New insight into the pectolite – serandite series: a single crystal diffraction study of $Na(Ca_{1.73}Mn_{0.27})[HSi_3O_9]$ at 293 and 100 K. *Z. Krist.*, **222**, 696–704.

Artioli, G., Geiger, C.A., Dapiaggi, M. (2003): The crystal chemistry of julgoldite-Fe^{3+} from Bombay, India, studied using synchrotron X-ray powder diffraction and ^{57}Fe Mössbauer spectroscopy. *Am. Mineral.*, **88**, 1084–1090.

Baur, W.H. (1980): Straight Si-O-Si bridging bonds do exist in silicates and silicon dioxide polymorphs. *Acta Cryst.*, **B36**, 2198–2202.

Biagioni, C. (2011): I silicati idrati di calcio: assetto strutturale e comportamento termico. PhD Thesis, University of Pisa, Italy.

Biagioni, C., Bonaccorsi, E., Merlino, S., Parodi, G.C., Perchiazzi, N., Chevrier, V., Bersani, D. (2010): Roumaite, $(Ca,Na,\square)_3(Ca,REE,Na)_4(Nb,Ti)(Si_2O_7)_2(OH)F_3$, from Rouma island, Los Archipelago, Guinea: a new mineral species related to dovyrenite. *Can. Mineral.*, **48**, 17–28.

Biagioni, C., Bonaccorsi, E., Merlino, S., Bersani, D., Forte, C. (2012): Thermal behaviour of tobermorite from N'Chwaning II mine (Kalahari Manganese Field, Republic of South Africa). II. Crystallographic and spectroscopic study of tobermorite 10 Å. *Eur. J. Mineral.*, **24**, 991–1004.

Biagioni, C., Merlino, S., Bonaccorsi, E. (2015): The tobermorite supergroup: a new nomenclature. *Mineral. Mag.*, **79**, 485–495.

Bonaccorsi, E. & Merlino, S. (2005): Modular microporous minerals: cancrinite-davyne group and C-S-H phases. *in* "Micro- and mesoporous mineral phases", Ferraris G., Merlino S. eds. , Rev. Mineral. Geochem., **57**, 241–290.

Britvin, S.N., Dolivo-Dobrovolsky, D.V., Krzhizhanovskaya, M.G. (2017): Software for processing the X-ray powder diffraction data obtained from the curved image plate detector of Rigaku RAXIS Rapid II diffractometer. *Zapiski RMO*, **146**, 104–107. (in Russian).

Cairncross, B., Beukes, N.J., Gutzmer, J. (1997): The Manganese Adventure. The South African Manganese Fields. Associated Ore & Metal Corp. Ltd, Johannesburg, South Africa.

Chukanov, N.V. (2014): Infrared spectra of mineral species: extended library. Springer-Verlag GmbH, Dordrecht, The Netherlands, 1716 p.

Chukanov, N.V. & Chervonnyi, A.D. (2016): Infrared spectroscopy of minerals and related compounds. Springer, Cham, Switzerland, 1109 p.

Chukanov, N.V., Kasatkin, A.V., Zubkova, N.V., Britvin, S.N., Pautov, L.A., Pekov, I.V., Varlamov, D.A., Bychkova, Y.V., Loskutov, A.B., Novgorodova, E.A. (2016): Tatarinovite, $Ca_3Al(SO_4)[B(OH)_4](OH)_6{\cdot}12H_2O$, a new ettringite-group mineral from the Bazhenovskoe deposit, Middle Urals, Russia, and its crystal structure. *Geol. Ore Dep.*, **58**, 653–665. (Special Issue: Zapiski RMO).

Czank, M. & Bissert, G. (1993): The crystal structure of $Li_2Mg_2[Si_4O_{11}]$, a loop-branched dreier single chain silicate. *Z. Krist.*, **204**, 129–142.

Erokhin, Y.V. (2017): Bazhenovskoe deposit (Central Urals, Russia): mineralogy of rodingites. *Mineral. Almanac*, **22**, 1–136.

Ferraris, G. & Ivaldi, G. (1988): Bond valence vs bond length in O···O hydrogen bonds. *Acta Crystallogr.*, **B44**, 341–344.

Gagné, O.C. & Hawthorne, F.C. (2015): Comprehensive derivation of bond-valence parameters for ion pairs involving oxygen. *Acta Crystallogr.*, **B71**, 562–578.

Gross, S. (1977): The mineralogy of the Hatrurim formation, Israel. Geological Survey of Israel Bulletin, **70**, 80 p.

Haring, M.M. & McDonald, A.M. (2014): Steedeite, $NaMn_2[Si_3BO_9](OH)_2$: characterization, crystal-structure determination, and origin. *Can. Mineral.*, **52**, 47–60.

—, — (2017): Nolzeite, $Na(Mn,\square)_2[Si_3(B, Si)O_9(OH)_2]{\cdot}2H_2O$, a new pyroxenoid mineral from Mont Saint-Hilaire, Québec, Canada. *Mineral. Mag.*, **81**, 183–197.

Heller, L. & Taylor, H.F.W. (1956): Crystallographic Data for the Calcium Silicates. H.M. Stationary Office, London, UK.

Hybler, J., Petříček, V., Jurek, K., Skála, R., Císařová, I. (1997): Structure determination of vistepite $SnMn_4B_2Si_4O_{16}(OH)_2$: isotypism with bustamite, revised crystallographic data and composition. *Can. Mineral.*, **35**, 1283–1292.

Kadiyski, M., Armbruster, T., Galuskin, E.V., Pertsev, N.N., Zadov, A.E., Galuskina, I.O., Wrzalik, R., Dzierzanowski, P., Kislov, E.V. (2008): The modular structure of dovyrenite, $Ca_6Zr[Si_2O_7]_2(OH)_4$: alternate stacking of tobermorite and rosenbuschite-like units. *Am. Mineral.*, **93**, 456–462.

Krzhizhanovskaya, M., Bubnova, R., Filatov, S. (2019): Crystalline borosilicates of alkaline and alkaline-earth metals: hierarchy, fundamental building blocks and thermal expansion. *Phys. Chem. Glass., Pt. B*, **60**. in press.

Kusachi, I., Henmi, C., Henmi, K. (1980): 10Å Tobermorite from Fuka, the town of Bitchu, Okayama Prefecture. *J. Mineral. Soc. Japan*, **14**, 314–322. (in Japanese).

—, —, — (1981): A new mineral, oyelite. Mineral. Soc. Japan, 1981 Annual Meeting Abstracts, p. 132 (in Japanese).

—, —, — (1984): An oyelite-bearing vein at Fuka, the town of Bitchu, Okayama Prefecture. *J. Japan. Assoc. Mineral., Petrol. Econ. Geol.*, **79**, 267–275.

Lykova, I.S., Varlamov, D.A., Chukanov, N.V., Pekov, I.V., Zubkova, N.V. (2018): Crystal chemistry of shuiskite and chromian pumpellyite-(Mg). *Eur. J. Mineral.*, **30**, 1133–1139.

Ma, Z.-S., Shi, N.-C., Mou, G.D., Liao, L.-B. (1999): Crystal structure refinement of suolunite and its significance to the cement techniques. *Chin. Sci. Bull.*, **44**, 2125–2130.

Maeshima, T., Noma, H., Sakiyama, M., Mitsuda, T. (2003): Natural 1.1 and 1.4 nm tobermorites from Fuka, Okayama Prefecture, Japan: chemical analysis, cell dimensions, ^{29}Si NMR and thermal behaviour. *Cement Concr. Res.*, **33**, 1515–1523.

Marincea, S., Bilal, E., Verkaeren, J., Pascal, M., Fonteilles, M. (2001): Superposed parageneses in the spurrite-, tilleyite- and gehlenite-bearing skarns from Cornet Hill, Apuseni Mountains, Romania. *Can. Mineral.*, **39**, 1435–1453.

Merlino, S., Bonaccorsi, E., Armbruster, T. (1999): Tobermorites: their real structure and order-disorder (OD) character. *Am. Mineral.*, **84**, 1613–1621.

—, —, — (2000): The real structures of clinotobermorite and tobermorite 9 Å: OD character, polytypes, and structural relationships. *Eur. J. Mineral.*, **12**, 411–429.

—, —, — (2001): The real structure of tobermorite 11 Å: normal and anomalous forms, OD character and polytypic modifications. *Eur. J. Mineral.*, **13**, 577–590.

Merlino, S., Bonaccorsi, E., Grabezhev, A.I., Zadov, A.E., Pertsev, N.N., Chukanov, N.V. (2009): Fukalite: an example of an OD structure with two-dimensional disorder. *Am. Mineral.*, **94**, 323–333.

Minakawa, T., Inaba, S., Noto, S. (1986): Oyelite from Suisho-dani, Ise, Mie Prefecture. *J. Japan. Assoc. Mineral., Petrol. Econ. Geol.*, **81**, 138–142. (in Japanese).

Murdoch, J. (1961): Crestmore, past and present. *Am. Mineral.*, **46**, 245–257.

Nagashima, M., Imaoka, T., Fukuda, C., Pettke, T. (2018a): Relationship between cation substitution and hydrogen-bond system in hydrous pyroxenoids with three-periodic single-chain of SiO_4 tetrahedra: pectolite, murakamiite, marshallsussmanite, serandite and tanohataite. *Eur. J. Mineral.*, **30**, 451–463.

Nagashima, M., Cametti, G., Armbruster, T. (2018b): Crystal chemistry of julgoldite, a mineral series of the pumpellyite group: re-investigation of Fe distribution and hydrogen-bonding. *Eur. J. Mineral.*, **30**, 721–731.

Ohashi, Y. & Finger, L.W. (1978): The role of octahedral cations in pyroxenoid crystal chemistry. I. Bustamite, wollastonite, and pectolite-schizolite-serandite series. *Am. Mineral.*, **63**, 274–288.

Pautov, L.A., Belakovskiy, D.I., Skala, R., Sokolova, E.V., Ignatenko, K.I., Mokhov, A.V. (1992): Vistepite, $Mn_5SnB_2Si_5O_{20}$, a new borosilicate of manganese and tin. *Zapiski VMO*, **121**, 107–112. (in Russian).

Pautov, L.A., Agakhanov, A.A., Karpenko, V.Yu., Uvarova, Yu.A., Sokolova, E., Hawthorne, F.C. (2019): Rinkite-(Y), $Na_2Ca_4YTi(Si_2O_7)_2OF_3$, a seidozerite-supergroup TS-block mineral from the Darai-Pioz alkaline massif, Tien-Shan mountains, Tajikistan: Description and crystal structure. *Mineral. Mag.*, **83**. DOI: 10.1180/mgm.2018.122.

Pekov, I.V., Chukanov, N.V., Filinchuk, Y.E., Zadov, A.E., Kononkova, N.N., Epanchintsev, S.G., Kaden, P., Kutzer, A., Göttlicher, J. (2013): Kasatkinite, $Ba_2Ca_8B_5Si_8O_{32}(OH)_3{\cdot}6H_2O$, a new mineral from the Bazhenovskoe deposit, the Central Urals, Russia. *Geol. Ore Dep.*, **55**, 558–566. (Special Issue: Zapiski RMO).

Sahl, K., Jones, P.G., Sheldrick, G.M. (1984): The crystal structure of davreuxite, $MnAl_6Si_4O_{17}(OH)_2$. *Am. Mineral.*, **69**, 783–787.

Sheldrick, G.M. (2015): Crystal structure refinement with SHELXL. *Acta Crystallogr.*, **C71**, 3–8.

Von Bezing, K.L., Dixon, R.D., Pohl, D., Cavallo, G. (1991): The Kalahari manganese field: an update. *Mineral. Rec.*, **22**, 279–297.

Zubkova, N.V., Pekov, I.V., Pushcharovsky, D.Yu., Zadov, A.E., Chukanov, N.V. (2012): The crystal structure of aklimaite, $Ca_4[Si_2O_5(OH)_2](OH)_4{\cdot}5H_2O$. *Z. Krist.*, **227**, 452–455.

Received 3 January 2019
Modified version received 22 February 2019
Accepted 5 March 2019